

## Electronic structures of perovskite BaTbO<sub>3</sub> studied by the LSDA +*U* method

This article has been downloaded from IOPscience. Please scroll down to see the full text article.

2005 J. Phys.: Condens. Matter 17 7963

(<http://iopscience.iop.org/0953-8984/17/50/014>)

View [the table of contents for this issue](#), or go to the [journal homepage](#) for more

Download details:

IP Address: 129.252.86.83

The article was downloaded on 28/05/2010 at 07:08

Please note that [terms and conditions apply](#).

# Electronic structures of perovskite BaTbO<sub>3</sub> studied by the LSDA + *U* method

Chunlan Ma<sup>1,2</sup>, Ling Ye<sup>1</sup> and Zhongqin Yang<sup>1</sup>

<sup>1</sup> Surface Physics Laboratory (National Key Laboratory), Fudan University, Shanghai 200433, People's Republic of China

<sup>2</sup> Department of Applied Physics, University of Science and Technology of Suzhou, Suzhou 215011, People's Republic of China

E-mail: [zyang@fudan.edu.cn](mailto:zyang@fudan.edu.cn)

Received 30 May 2005, in final form 11 October 2005

Published 2 December 2005

Online at [stacks.iop.org/JPhysCM/17/7963](http://stacks.iop.org/JPhysCM/17/7963)

## Abstract

The electronic and magnetic properties of BaTbO<sub>3</sub> are studied by using the local-spin density approximation method where on-site Coulomb interaction *U* is included. The ground magnetic phase is found to be G-type antiferromagnetic with lattice constant of 4.278 Å, which is consistent with experimental results. The states of Ba in the compound show obvious ionic characteristic, while very strong hybridization between Tb 4f and O 2p orbitals is found in the compound. The on-site Coulomb interaction *U* is found to have significant influences on the state distribution of Tb 4f. With the increase of *U*, most of the spin-up and spin-down states of Tb 4f move away from the Fermi level drastically, giving rise to the change of band gap of the compound and the variation of magnetic moment of Tb ions. The optimized value of *U* is determined to be 4.0 eV, and the corresponding band gap of BaTbO<sub>3</sub> is 0.61 eV, which seems to be a narrow gap semiconductor rather than a good insulator.

## 1. Introduction

BaTbO<sub>3</sub> is a kind of ABO<sub>3</sub> perovskite material containing tetravalent rare earth ions. The simple perovskite BaTbO<sub>3</sub> has been suggested to be a candidate for the new insulating materials for high-*T*<sub>c</sub> superconductor devices due to the compatibility of YBa<sub>2</sub>Cu<sub>3</sub>O<sub>7-x</sub> (YBCO) and BaTbO<sub>3</sub>, and even a large doping of YBCO with Ba or Tb due to the interdiffusion at the YBCO/BaTbO<sub>3</sub> interface does not cause a noticeable reduction of *T*<sub>c</sub> [1]. In addition, BaTbO<sub>3</sub> doped with trivalent In ions at the B-sites has caused great interest because of its potential applications in solid-state fuel cells, steam electrolyzers and humidity sensors [2]. Several groups have performed experimental studies on the crystal structures [3–8] and magnetic properties [2, 4, 6] of BaTbO<sub>3</sub>. Although the crystal structures of BaTbO<sub>3</sub> found by experiments could be rhombohedral [3–5], orthorhombic [6] or tetragonal [7, 8], they are basically slightly

distorted cubic structures since the tolerance factor defined by  $t = \frac{(r_A+r_B)}{\sqrt{2}(r_B+r_O)}$  is very close to unity (0.985) for BaTbO<sub>3</sub> [7]. The magnetic phase found is antiferromagnetic with spins in alternate (111) planes oppositely aligned, i.e., G-type AFM [3]. However, in spite of the above experimental studies, there has been no theoretical electronic structure investigation on BaTbO<sub>3</sub> up to the present, which is indispensable for understanding the basic electronic properties of this material.

In this work, we present a systematic study of the electronic structures and magnetic properties of BaTbO<sub>3</sub> by using the local density functional approximation (LSDA) method. Since the LSDA cannot describe strongly correlated systems which contain transition metals or rare earth elements with partially filled d or f shells [9, 10], we considered the on-site Coulomb interaction  $U$  on Tb 4f states in the calculation to improve the results, namely, using the LSDA +  $U$  method [11–13] to study the electronic structures of the compound. Although many transition metal compounds containing 3d local electrons have been well described by LSDA +  $U$  [14–16], the systems containing localized 4f electrons were rarely studied by LSDA +  $U$  [17, 18] due to the complexity of the band structure. Our theoretical calculation confirms that the ground magnetic phase of BaTbO<sub>3</sub> is G-AFM with lattice constant of 4.278 Å, consistent with the experimental results [3, 8]. The on-site Coulomb interaction  $U$  has significant influences on the electronic density of states and energy band gap of BaTbO<sub>3</sub> as well as the magnetic moment of Tb ions. The calculated magnetic moment approaches the measured one at  $U = 4.0$  eV. Correspondingly, the energy gap of BaTbO<sub>3</sub> reaches its maximum of 0.61 eV. This energy gap value and the calculated energy band diagram illustrate that BaTbO<sub>3</sub> would be a type of indirect gap semiconductor rather than an insulator as suggested by previous work [1].

## 2. Calculation model and method

As we have mentioned above, the crystal structure of BaTbO<sub>3</sub> is a slightly distorted cubic structure with only 0.26% deviation of the lattice parameter along the  $c$  axis, and 0.45% along the  $a$  axis with respect to  $b$ , which can be deduced from [8]. To simplify the calculation, we brush aside the negligible distortion and assume a cubic structure. For G-AFM BaTbO<sub>3</sub>, there are two kinds of Tb (labelled as Tb<sub>1</sub> and Tb<sub>2</sub>) possessing opposite magnetic moment directions indicated by up and down arrows on the atoms in the inset of figure 1. The compound with G-AFM structure forms a face-centred cubic structure.

The calculations were done by using the linear muffin-tin orbitals method within the atomic-sphere approximation (LMTO-ASA) [19]. It has been verified that the structures are sufficiently well packed, thus no empty sphere needs to be inserted in the unit cell. Within the atomic spheres, the basis functions, the charge density and potential were expanded in spherical harmonics and radial functions. The states of Ba 6s, 5p, 5d, 4f, Tb 6s, 5p, 5d, 4f, and O 2s, 2p have been taken as the basis sets in the calculation. The states of Ba 5s and Tb 5s were treated as semicore ones. The radial part of the basis was obtained by solving Kohn–Sham equation in which semi-relativistic corrections were incorporated. The local exchange–correlation potential of Vosko–Wilk–Nussair [20] type was employed. The integration over the Brillouin zone was made with the tetrahedron method.

We employed the LSDA +  $U$  method proposed by Anisimov *et al* [11], in which the orbital-dependent one-electron potential is written as

$$V_{mm'}^\sigma = \sum_{\{m\}} \{ \langle m, m'' | V_{ee} | m', m''' \rangle n_{m''m'''}^{-\sigma} - (\langle m, m'' | V_{ee} | m', m''' \rangle - \langle m, m'' | V_{ee} | m''', m' \rangle) n_{m''m'''}^\sigma \} - U(N - \frac{1}{2}) + J(n^\sigma - \frac{1}{2})$$

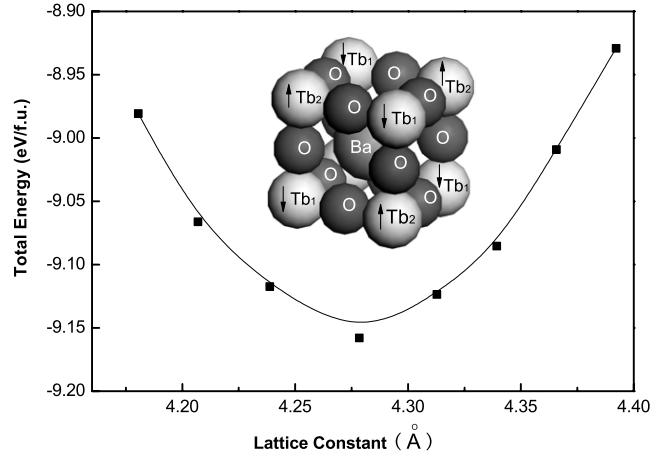


**Figure 1.** Total energy per formula unit (f.u.) of G-AFM BaTbO<sub>3</sub> versus lattice constant by using the standard LSDA method. The arrangement of atoms in the structure is shown in the inset, where the large ball at the centre represents Ba atom. Due to the AFM coupling of Tb ions, there are two kinds of Tb ions (Tb<sub>1</sub> and Tb<sub>2</sub>) with opposite spin directions in the structure. The up and down arrows on Tb atoms in the inset indicate the spin up and down directions, respectively.

where  $V_{ee}$  are the screened Coulomb interactions among the  $nl$ -electrons ( $n$  denotes the main quantum number, and  $l$  denotes the orbital quantum number), and  $U$ ,  $J$  are screened Coulomb and exchange parameters, respectively. The matrix elements can be expressed in terms of complex spherical harmonics and effective Slater integrals  $F^k$  [21] as

$$\langle m, m'' | V_{ee} | m', m''' \rangle = \sum_k a_k(m, m', m'', m''') F^k$$

where  $0 \leq k \leq 2l$  and

$$a_k(m, m', m'', m''') = \frac{4\pi}{2k+1} \sum_{q=-k}^k \langle lm | Y_{kq} | lm' \rangle \langle lm'' | Y_{kq}^* | lm''' \rangle.$$

For  $f$  electrons, the relations between the parameters used are  $U = F^0$ ,  $J = (286F^2 + 195F^4 + 250F^6)/6435$ ,  $F^4 = 0.625F^2$ , and  $F^6 = 0.5F^2$  [22]. Thus, if the averaged parameters  $U$  and  $J$  are known,  $F^0$ ,  $F^2$ ,  $F^4$ ,  $F^6$  and also the matrices can be obtained through the above relations. The average Coulomb  $U$  parameter for Tb ions was taken to be 3.0, 4.0 and 5.0 eV. The exchange parameter  $J$  was fixed at 0.8 eV.

### 3. Results and discussion

We calculate the total ground-state energies of paramagnetic (PM), ferromagnetic (FM), and G-AFM BaTbO<sub>3</sub> versus lattice constant by using standard LSDA method. It is found that PM and FM BaTbO<sub>3</sub> have much higher total energies than that of G-AFM BaTbO<sub>3</sub>, by 8.50 and 0.15 eV/formula unit, respectively. Thus our calculation agrees very well with the experimental work that G-AFM is observed to be the most stable magnetic structure for BaTbO<sub>3</sub> [3]. The calculated total energy as a function of lattice constant for G-AFM BaTbO<sub>3</sub> is shown in figure 1, in which the total energy of PM BaTbO<sub>3</sub> is taken as energy zero. From the calculation an equilibrium lattice constant of 4.278 Å is obtained. This value is very close to the previous experimental values of 4.285 Å [3] and 4.297 Å [8].

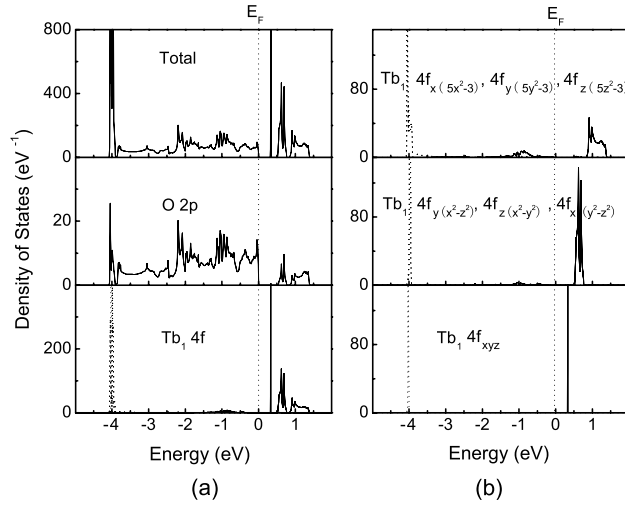


**Figure 2.** (a) Total and partial densities of states (O 2p and Tb<sub>1</sub> 4f) of G-AFM BaTbO<sub>3</sub> calculated by using the LSDA. (b) The corresponding *m*-dependent partial densities of states of Tb<sub>1</sub> 4f of G-AFM BaTbO<sub>3</sub>. The solid and dotted curves represent spin-up and spin-down bands, respectively. The Fermi level is chosen as the energy zero.

The electronic structures of the G-AFM BaTbO<sub>3</sub> are studied first by using the standard LSDA in order to compare with those from LSDA + *U*. The total density of states (TDOS) obtained by using LSDA is shown in the upper panel of figure 2(a), where the energy scale is with respect to the Fermi level. An obvious ionic character of Ba is obtained in the calculation (not shown in the figure): Ba 5p is deeply occupied at −12.0 eV and Ba 6s, 5d, 4f are all unoccupied above 4.0 eV. The partial DOSs (PDOSs) of O 2p and Tb<sub>1</sub> 4f are shown in the middle and lower panels of figure 2(a). One can see that the valence band near *E<sub>F</sub>* is mainly contributed by O 2p. The sharp peaks around −4.0 eV is due to the hybridization of O 2p and Tb 4f, and the peak at 0.33 eV is due to unoccupied Tb 4f. The peaks from 0.5 to 1.4 eV originate from mixed unoccupied Tb 4f and O 2p states.

In the PDOS of Tb<sub>1</sub> 4f, it can be seen that the occupied Tb<sub>1</sub> 4f orbitals are populated by spin-down electrons. Actually, the PDOS of spin-up Tb<sub>1</sub> 4f is the same as spin-down Tb<sub>2</sub> 4f (dotted line) and that of spin-down Tb<sub>1</sub> 4f is the same as spin-up Tb<sub>2</sub> 4f (solid line) due to the AFM structure of the compound. So it is the spin-up electrons that occupies at Tb<sub>2</sub> 4f states. O 2p, which should be fully occupied, has some unoccupied states due to its strong hybridization with Tb 4f.

To analyse the electronic structures further, we show the PDOS of Tb<sub>1</sub> 4f corresponding to different magnetic quantum number (*m*-dependent PDOS) in figure 2(b). It can be seen that the 4f orbitals consist of two triply degenerate orbitals  $4f_{x(5x^2-3)}$ ,  $4f_{y(5y^2-3)}$ ,  $4f_{z(5z^2-3)}$  (in the upper panel) and  $4f_{y(x^2-z^2)}$ ,  $4f_{z(x^2-y^2)}$ ,  $4f_{x(y^2-z^2)}$  (in the middle panel) and one non-degenerate orbital  $4f_{xyz}$  (in the lower panel) due to the cubic symmetry. The PDOS around −1 eV for  $4f_{x(5x^2-3)}$ ,  $4f_{y(5y^2-3)}$ ,  $4f_{z(5z^2-3)}$  orbitals shows a strong hybridization with the O 2p orbital. The lowest-lying unoccupied peak at 0.33 eV is formed by Tb  $4f_{xyz}$ . The magnitude difference of spin-up and spin-down occupations in Tb<sub>1</sub> 4f causes a net magnetic moment on Tb<sub>1</sub> ion with the value of 5.76  $\mu_B$ , which is smaller to certain extent than the experimental value of 6.50  $\mu_B$  [6].

The electronic structures obtained by using LSDA + *U* are shown in figure 3 with *U* being 3.0, 4.0, and 5.0 eV. As a comparison, the result of the LSDA is also given in the upper panel.

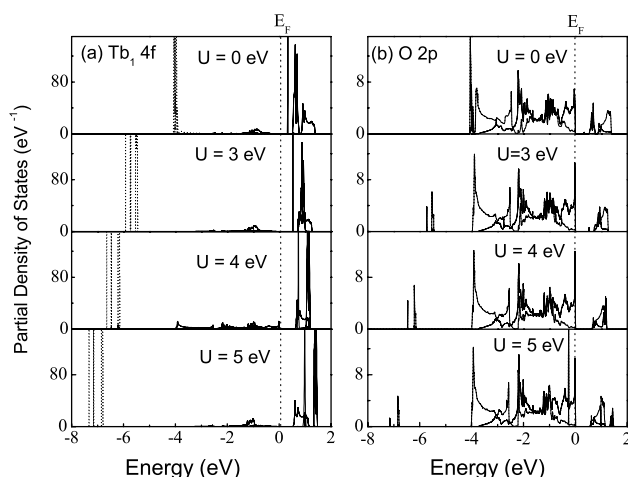


**Figure 3.** The partial densities of states of (a) Tb<sub>1</sub> 4f and (b) O 2p as a function of *U* varying from 3.0 to 5.0 eV. The solid and dotted curves represent spin-up and spin-down bands, respectively. The Fermi level is chosen as the energy zero. The results obtained without considering the on-site Coulomb interaction are also given for comparison.

**Table 1.** Energy gap and magnetic moment calculated by using LSDA and LSDA + *U* (*J* = 0.8 eV).

Method	LSDA		LSDA + <i>U</i>		
<i>U</i> (eV)			3.0	4.0	5.0
Energy gap (eV)	0.32	0.51	0.61	0.53	
Magnetic moment ( $\mu_B$ )	5.76(2)	5.81(9)	5.82(8)	5.82(7)	

The main effect of *U* on the Tb 4f orbitals is to separate further the spin-up and spin-down energy levels. The O 2p levels are basically unaffected by *U* except those hybridized with Tb 4f orbitals. One can see that with the increase of *U*, Tb 4f states mainly move apart from the Fermi level significantly, except the unoccupied triply degenerate orbitals  $4f_{x(5x^2-3)}$ ,  $4f_{y(5y^2-3)}$ ,  $4f_{z(5z^2-3)}$ , which move downwards slightly. This may be ascribed to the stronger hybridization between the states of  $4f_{x(5x^2-3)}$ ,  $4f_{y(5y^2-3)}$ ,  $4f_{z(5z^2-3)}$  and O 2p than that of other 4f states and O 2p due to similar distribution to certain extent of  $4f_{x(5x^2-3)}$ ,  $4f_{y(5y^2-3)}$ ,  $4f_{z(5z^2-3)}$  and O 2p in real space. As a result, when *U* is small, the lowest-lying unoccupied state is Tb  $4f_{xyz}$ , which moves upward with the increase of *U*. If this narrow energy level is considered to be the bottom of conduction band, the band gap of BaTbO<sub>3</sub> increases with *U*. When *U* > 4.0 eV, the downward shifted orbitals  $4f_{x(5x^2-3)}$ ,  $4f_{y(5y^2-3)}$ ,  $4f_{z(5z^2-3)}$  are located below the upward shifted orbital  $4f_{xyz}$  and become the bottom of the conduction band, so the gap decreases slightly with the increase of *U*. The gap is 0.61 eV at the critical *U* of 4.0 eV. It is noticeable that the magnetic moment of the Tb ion has the same variation trend with the gap. Table 1 shows the energy gap and magnetic moment varying with *U* being 3.0, 4.0, and 5.0 eV. When *U* = 4.0 eV, the magnetic moment reaches a maximum of 5.83  $\mu_B$ , which is closest to the experimental value [6]. Thus we suggest the Coulomb interaction *U* of Tb in BaTbO<sub>3</sub> should be chosen as 4.0 eV. Up to now, there are very few works that treat the localized f orbitals by using the LSDA + *U* method. The optimized value of Hubbard *U* obtained in this work is the same as that of Pu 5f obtained in previous work [18].

The calculated band structures by the LSDA and LSDA + *U* methods for G-AFM BaTbO<sub>3</sub> along the high-symmetry directions in the Brillouin zone are shown in figure 4. With the LSDA

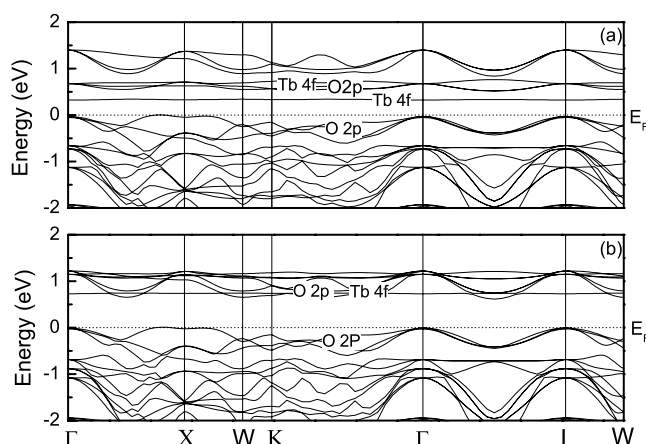


**Figure 4.** The band structures of G-AFM BaTbO<sub>3</sub> obtained within (a) LSDA and (b) LSDA +  $U$  ( $U = 4.0$  eV,  $J = 0.8$  eV).

calculation, the energy separation between the O 2p valence band and the lowest-lying empty states Tb 4f<sub>xyz</sub> is 0.32 eV. If the latter could be viewed as the conduction band of BaTbO<sub>3</sub>, a direct band is formed. When Coulomb interaction is considered, the unoccupied 4f<sub>xyz</sub> state moves upwards, and the hybridization states of Tb 4f<sub>x(5x<sup>2</sup>-3)</sub>, 4f<sub>y(5y<sup>2</sup>-3)</sub>, 4f<sub>z(5z<sup>2</sup>-3)</sub> and O 2p form the bottom of conduction band. It is also noted that the band structure varies from a direct band gap to an indirect one with an energy gap of 0.61 eV. The valence band maximum is located at the  $\Gamma$  point, while the conduction band minimum is located along the  $\Gamma$ -X or  $\Gamma$ -L direction in the Brillouin zone. This indirect band gap does not seem large enough to make BaTbO<sub>3</sub> a good insulating material for high- $T_c$  superconductor devices as claimed by [1].

#### 4. Conclusion

The electronic structures of BaTbO<sub>3</sub> has been studied by using LSDA and LSDA +  $U$  methods. By calculating the total energies of PM, FM and G-AFM BaTbO<sub>3</sub>, the ground magnetic phase of the compound is found to be G-AFM with the lattice constant of 4.278 Å, consistent with the experimental results. The inclusion of Hubbard  $U$  of Tb ions gives significant effects on the electronic density of states, energy band structure, and the magnetic moment. The optimized value of  $U$  in BaTbO<sub>3</sub> is suggested to be 4.0 eV from our calculation. The energy band of BaTbO<sub>3</sub> is found to be an indirect one with a gap of 0.61 eV.

#### Acknowledgments

This work was supported by the National Natural Science Foundation of China under the Grant No 10304002 and the Fudan High-end Computing Centre.

#### References

- [1] Hojczyk R, Jia C L, Poppe U and Urban K 1997 *Physica C* **282-287** 731
- [2] Arons R R 1998 *J. Magn. Magn. Mater.* **177-181** 869
- [3] Jacobson A J, Tofield B C and Fender B E F 1972 *Acta Crystallogr. B* **28** 956
- [4] Tofiel B C, Jacobson A J and Fender B E F 1972 *J. Phys. C: Solid State Phys.* **5** 2887

- [5] Banks E, La Place S J, Kunnmann W, Corliss L M and Hastings J M 1972 *Acta Crystallogr. B* **28** 3429
- [6] Tezuka K, Hinatsu Y, Shimojo Y and Morii Y 1998 *J. Phys.: Condens. Matter* **10** 11703
- [7] Fu W T, Visser D, Knight K S and IJdo D J W 2002 *J. Solid State Chem.* **165** 393
- [8] Fu W T, Visser D, Knight K S and IJdo D J W 2004 *J. Solid State Chem.* **177** 1667
- [9] Sarma D D, Shanthi N, Barman S R, Hamada N, Sawada H and Terakura K 1995 *Phys. Rev. Lett.* **75** 1126
- [10] Pickett W E and Singh D J 1996 *Phys. Rev. B* **53** 1146  
Pari G, Jaya S M, Subramoniam G and Asokamani R 1995 *Phys. Rev. B* **51** 16575
- [11] Anisimov V I, Zaanen J and Andersen O K 1991 *Phys. Rev. B* **44** 943  
Anisimov V I, Solovyev I V, Korotin M A, Czyżyk M T and Sawatzky G A 1993 *Phys. Rev. B* **48** 16929
- [12] Czyżyk M T and Sawatzky G A 1994 *Phys. Rev. B* **49** 14211
- [13] Lichtenstein A I, Zaanen J and Anisimov V I 1995 *Phys. Rev. B* **52** R5467
- [14] Fujimori A and Minami F 1984 *Phys. Rev. B* **30** 957  
van Elp J, Potze R H, Eskes H, Berger R and Sawatzky G A 1991 *Phys. Rev. B* **44** 1530
- [15] Korotin M A, Ezhov S Yu, Solovyev I V, Anisimov V I, Khomskii D I and Sawatzky G A 1996 *Phys. Rev. B* **54** 5309  
Solovyev I, Hamada N and Terakura K 1996 *Phys. Rev. B* **53** 7158
- [16] Yang Z Q, Huang Z, Ye L and Xie X D 1999 *Phys. Rev. B* **60** 15674
- [17] Huang Z, Ye L, Yang Z Q and Xie X 1975 *Phys. Rev. B* **61** 12786
- [18] Savrasov S Y, Kotliar G and Abrahams E 2001 *Nature* **410** 794
- [19] Andersen O K 1975 *Phys. Rev. B* **12** 3060  
Andersen O K, Pawłowska Z and Jepsen O 1986 *Phys. Rev. B* **34** 5253  
Skriver H L 1984 *The LMTO Method* (Berlin: Springer)
- [20] Vosko S H, Wilk L and Nusair M 1980 *Can. J. Phys.* **58** 1200  
Ceperly D M and Alder B J 1980 *Phys. Rev. Lett.* **45** 566  
Ceperly D M and Alder B J 1972 *Phys. Rev. Lett.* **5** 1629
- [21] Judd B R 1963 *Operator Techniques in Atomic Spectroscopy* (New York: McGraw-Hill)
- [22] Anisimov V I, Aryasetiawanz F and Lichtenstein A I 1997 *J. Phys.: Condens. Matter* **9** 770